Struvite infection calculi in dogs: Problems with urinary calculus identification, and the value of the results

John Dunlevey[a*] **and Michael Laing**[b]

IDENTIFYING THE CRYSTALLINE COMPONENTS of a urinary calculus is a valuable aid to correct diagnosis, and subsequent treatment of the underlying cause of the problem. Calculus formation is often an end product brought about by urine with a high concentration of insoluble material causing bladder irritation. This promotes bacterial infection by *Proteus,* which not only raises the pH in the bladder and generates ammonia, but also provides sites for mineral nucleation and crystal growth. Treating the infection and removing the stone will not necessarily cure the disorder. Correct identification of a calculus as struvite and even its potassium analogue can be critical in choice of curative protocols, but this is not always straightforward. Our experience with 'problem calculi' is described.

Introduction

We have been systematically analysing urinary calculi by the X-ray powder diffraction method since 1978, in both humans and domestic animals.[1–3] The formation of a struvite calculus is normally due to the presence of ammonia and a raised pH in the urine, caused by infection. We have found over the past four years that some struvite bladder calculi from dogs display abnormal intensity peak patterns that are not immediately identifiable, even through the *d*-spacings of the planes appear to be generally correct.[4] These discrepancies are so large as to be of significance and warrant reporting.

Experimental

X-ray powder diffraction (XRD) patterns were recorded with cobalt K_α radiation (λ = 1.7889 Å) as described in ref. 1. A selection of observed patterns is shown in Fig. A (see supplementary material online), and a list of the *d*-spacings and the relative intensities of diffraction peaks are given in Table 1 (online). The calculi were also analysed for the presence of various chemical elements using the EDAX technique on a JEOL scanning electron microscope, because the presence of calcium is indicative of amorphous hydroxyl apatite, which often exists as an amorphous solid and is therefore not evident in the XRD scan.

Results

Typical analytical data are presented in Fig. B (online). The results from a collection of struvite stones are given in Fig. 1 and Fig. A (online). A comparison of the observed peak intensities (Table 1) with the standard pattern[4] shows quite clearly that few of the samples (e.g. A–D, Table 1) give the 'normal' intensity distribution. For convenience, the diffraction patterns in Table 1 are grouped by the common most intense diffraction peak, which arises from the 4.26, 5.60, 2.69 and 4.13 Å planes. The powder diffraction patterns in Fig. A illustrate the problem, and it is hard to believe that all were generated from the same crystalline compound. Thus, there will be a major problem if one uses the set of four strongest lines as the primary criterion (Hanawaldt search) for identifying the 'unknown'. However, there are always the same groups of *d*-spacings with strong reflections {5.90, 5.60, 5.38}; {4.26, 4.13}; {2.80, 2.69, 2.66}, but the strongest may occur in any of the three groups (compare the examples in Table 1: Suzy 5.60 Å [G]; Dallas 4.26 Å [D]; Cleo 2.80 Å [S] and Cheeky 2.69 Å [U]).

The problem of potassium

The most commonly occurring mineral species in calculi from dogs is struvite, an ammonium magnesium phosphate hydrate [$NH_4MgPO_4{\cdot}6H_2O$]. However, we were surprised when potassium was detected by EDAX in several of the stones. It transpires that a well-defined potassium analogue [$KMgPO_4{\cdot}6H_2O$] of struvite exists, where K^+ replaces the NH_4^+ ammonium cations. These two compounds are isostructural,[6,7] with the existence of a complete isomorphous series from 100% K^+ to 100% NH_4^+ struvite.[6] This ion replacement is possible, as the ionic radii of K^+ and NH_4^+ are almost identical[8] (1.52 vs 1.51 Å).

It is evident that when the struvite (infection) calculus forms and is growing, any potassium present in the urine can be incorporated into the crystal structure of the stone. This potassium can be detected by EDAX, but can also show itself by subtle effect on all the *d*-spacings (those of ideal pure struvite are about 2% greater than

---

[a] School of Earth Science, University of KwaZulu-Natal, Durban 4041, South Africa.

[b] School of Pure and Applied Chemistry, University of KwaZulu-Natal, Durban.

*Author for correspondence.
E-mail: dunleveyj@ukzn.ac.za

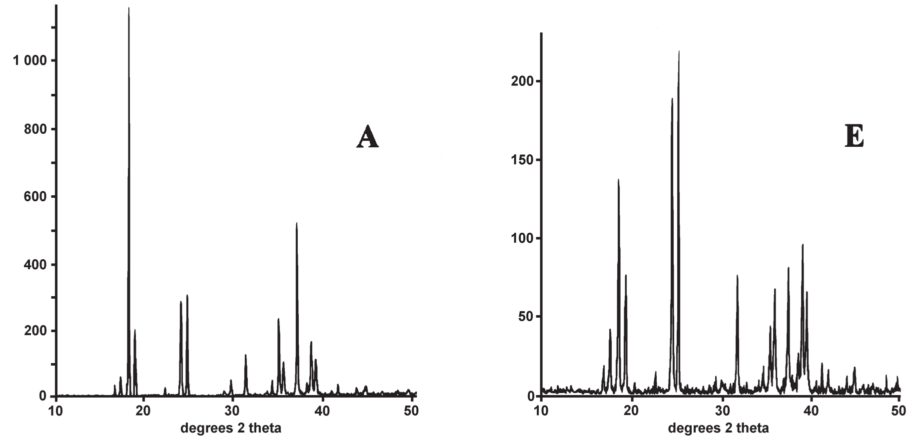

Fig. 1. Two examples of observed X-ray powder diffraction patterns of struvite calculi. In all cases, the *d*-spacings (values of 2θ) are the same for the important lines, but the relative intensities vary greatly. In A the peak at 19° is far higher than the pair at 24° 2θ. In E the situation is reversed; the pair at 24° is the strongest. These anomalous intensities can make identifying the calculus as struvite difficult if only the three or four strongest lines are used as the criterion in searching the Powder Diffraction File. Using the seven strongest lines, and ignoring the relative intensities, normally will identify the species as struvite. Neither scan has obvious high backgrounds, nor are there the broad peaks due to poorly crystalline hydroxyl apatite (2.81–2.72 Å; 37–38° 2θ). Six additional scans of this kind are reproduced in Fig. A online.

those of the potassium analogue). Table 2 (see supplementary material online) compares the unit cell dimensions and important *d*-spacings of the two crystalline compounds. It is clear that material that contains both K^+ and NH_4^+ cations will have *d*-spacings of intermediate size; but the effect is very small, with differences being detectable only in the second decimal place of the *d*-spacing. Unfortunately, this level of precision is not usually attainable during typical routine powder diffraction analysis of calculi samples.

Figures C and D (both online) are projections of the crystal structures along the *b*-axis. It is evident that the site occupied by the K^+ and NH_4^+ ions lies on the 110, 020, 021, 200 and 130 planes and diffraction from these should be most affected by the replacement of NH_4^+ by K^+ (Table 2).

An unusual result

Calcium is regularly found in calculi,[2,3] most commonly as the phosphate [hydroxyl apatite $Ca_5(PO_4)_3(OH)$] and less often as an oxalate [monohydrate whewellite $CaC_2O_4{\cdot}H_2O$; dihydrate weddelite $CaC_2O_4{\cdot}2H_2O$]. The struvite calculi from the dog named Rambo consist of two types of material: (i) dark, hard, containing only magnesium (typical struvite); (ii) softer, granular containing some calcium. The intensities of the diffraction peaks from the type (ii) material were distinctly weaker than those from the type (i) material, indicating that type (ii) was less crystalline, that is, the internal structure was not as regular as in the ideal struvite structure. Close analysis of the XRD powder pattern reveals a broad background hump between 35° and 39° 2θ (*d*-spacing between 2.72 and 2.81 Å) and indicates the presence of amorphous hydroxyl apatite. The presence of apatite in a calculus is indicative of hyperparathyroidism.[1,2]

Discussion

The anomalous intensity patterns are immediately obvious and can arise from several sources. Examples are: orientation effects from abnormal crystal shape due to the mode of crystal growth;[10] particle size effects; degree of pressure during grinding of the sample; loss of water from the crystal structure; isomorphous replacement of some magnesium by calcium, or ammonium by potassium. Our results show that there is no direct correlation between calcium content and the magnitude or pattern of anomalies in the X-ray powder patterns of the struvite in these stones. Where calcium is detected by EDAX or XRF, it is usually associated with solid, amorphous, hydroxyl apatite.

The results show that there are two types of complementary information obtainable. X-Ray powder diffraction immediately identifies the calculus as a 'struvite infection' stone, and thus the patient can be treated appropriately. However, identifying the presence of calcium and/or potassium by EDAX can give an important indication of the underlying problem. For example, calcium, present as amorphous hydroxyl apatite, may indicate a malfunction of the dog's parathyroid gland. If a dog presents a bladder calculus, it may be of value to routinely check the urine for pH as well as for ammonia, which may indicate infection. An excessively high result for potassium may be an indicator for the underlying cause of calculus formation.

Conclusions

We offer the above experiences as a salutary example to other researchers who may be using the X-ray powder diffraction technique. Do not be misled (as we were initially) by 'missing lines' and 'wrong intensities'. These anomalies are not uncommon, and their identification may provide valuable hints of minor but important complexities associated with the condition that generated the stone. Should any readers wish to have urinary calculi analysed by XRD (canine, feline or human), we would be pleased to have them as contributors to this continuing research project.

We thank the University of KwaZulu-Natal for supporting this research project and providing access to the XRD and SEM EDAX equipment. We acknowledge the assistance of the late F. Graham, and D. Rabie (Umbilo Veterinary Clinic) as well as the many pet owners who have donated the calculi removed from their dogs.

Received 6 June. Accepted 20 August 2008.

---

1. Gray D., Laing M., Nel F. and Naude J.H. (1982). Composition of urinary calculi collected in the Durban area. *S. Afr. Med. J.* **61**, 121–125.
2. Laing M., Kerr A. and Nel F. (1993). Fifteen years and 5000 X-ray patterns later: renal stone analysis at the University of Natal, Durban. *S. Afr. J. Sci.* **89**, 528–530.
3. Laing M. and Dunlevey J. (2000). A novel urinary calculus from *Felis catus*. *S. Afr. J. Sci.* **96**, 220–221.
4. JCPDS (1997). Powder Diffraction File 15–762. ICDD, Walnut Street, Philadelphia, PA.
5. Banks E., Chianelli R. and Korenstein R. (1975). Crystal chemistry of struvite analogs of the type $MgMPO_4{\cdot}6H_2O$ ($M^+ = K^+, Rb^+, Cs^+, Tl^+, NH_4^+$). *Inorg. Chem.* **14**, 1634–1639.
6. Mathew M. and Schroeder L.W. (1979). Crystal structure of a struvite analogue $MgKPO_4{\cdot}6H_2O$. *Acta Cryst.* **B35**, 11–13.
7. Whitaker A. and Jeffery J.W. (1970). The crystal structure of struvite $MgNH_4PO_4{\cdot}6H_2O$. *Acta Cryst.* **B26**, 1429–1440.
8. Huheey J.E., Keiter E.A. and Keiter R.L. (1993). *Inorganic Chemistry*, 4th edn. HarperCollins, New York.
9. JCPDS (1997). Powder Diffraction File patterns 15–762 and 35–812. ICDD, Walnut Street, Philadelphia, PA.
10. Abbona F., Calleri M. and Ivaldi G. (1984). Synthetic struvite $MgNH_4PO_4{\cdot}6H_2O$ correct polarity and surface features of some complementary forms. *Acta Cryst.* **B40**, 223–227.

This article is accompanied by supplementary analytical and crystallographic results in tabular and graphical form online at www.sajs.co.za

Supplementary material to:

Dunlevey J. and Laing M. (2008). Struvite infection calculi in dogs: Problems with urinary calculus identification, and the value of the results. *S. Afr. J. Sci.* **104**, 471–472.

Table 1. A comparison of the X-ray powder diffraction peaks of synthetic struvite (ICDD data file 15-762) with those struvite calculi recovered from 21 pet dogs.

No.	*d* (Å)	I_{rel}	A	B	C	D	E	F	G	H	I	J	K	L	M	N	O	P	Q	R	S	T	U
1	6.13	8	6	10	9	11	7	20	11	3	13	7	1	2	3	4	1	11	4	7	2	3	13
2	6.90	40	10	30	18	35	12	<1	40	10	24	24	9	5	10	27	5	14	18	4	11	6	15
3	5.60	60	91	97	55	79	100	100	100	100	100	100	100	100	100	96	41	58	60	70	28	77	82
4	5.38	25	59	51	36	39	50	48	38	24	34	25	15	14	21	45	10	34	29	3	14	24	63
5	4.60	6	3	6	6	7	7	9	10	6	4	4	2	2	<1	2	<1	4	6	<1	1	2	1
6	2.26	100	100	100	100	100	44	24	88	45	79	71	42	22	37	59	20	67	87	9	25	27	70
7	4.13	40	39	78	36	71	24	18	57	73	57	29	19	25	42	20	6	68	100	16	5	24	49
8	3.47	12	2	6	13	5	3	<1	8	3	4	4	1	4	2	10	3	3	3	<1	2	4	5
9	3.29	25	28	18	27	30	7	3	30	25	28	11	4	8	6	8	100	11	26	1	6	6	18
10	3.02	14	4	8	19	14	2	<1	11	8	9	7	3	3	<1	1	<1	3	4	2	1	3	12
11	2.96	25	13	21	<1	<1	10	<1	16	6	15	21	<1	<1	3	<1	3	13	19	4	<1	3	<1
12	2.92	55	15	27	34	40	34	12	29	15	24	32	20	8	8	28	6	17	31	<1	18	9	32
13	2.80	35	45	34	35	28	22	19	59	27	40	57	13	38	47	22	18	21	31	100	100	15	25
14	2.69	50	36	42	46	65	58	14	55	30	43	30	5	12	20	18	29	100	43	8	8	100	100
15	2.66	45	8	17	22	23	22	<1	42	8	24	18	41	8	9	100	36	18	29	<1	11	6	18
16	2.35	12	2	5	4	9	4	<1	16	3	5	<1	1	<1	3	<1	33	4	7	2	2	2	5

d(Å) = *d*-spacing and I_{rel} = intensity, data from JCPDS–ICDD (1993) database; struvite data file 15-762.
Sources: A, Suzie H; B, Matie; C, Bugsie; D, Dallas; E, Rambo I; F, Rambo II; G, Suzy 3; H, Minke; I, Wishbone (outer); J, Mikis; K, Jamie; L, Bayete; M, Bonnie; N, Kaylee A; O, Kaylee B; P, Suzy N; Q, Thompson; R, Minky (outside); S, Cleo; T, Wishbone; U, Cheeky.

Table 2. Comparison of the unit cell dimensions and X-ray powder diffraction patterns for struvite ($NH_4MgPO_4 \cdot 6H_2O$) and the potassium analogue ($KMgPO_4 \cdot 6H_2O$) in which the K^+ has replaced the NH_4^+ ammonium ion. Data from JCPDS–ICDD (1993) database, struvite data file 15–762, potassium analogue data file 35–812. Note the *hkl* indices are those given in the Powder File and should be transposed to read *hlk* for the published cell in 6 and 7.

Unit cell dimensions

	a (Å)	*b* (Å)	*c* (Å)	*V* (Å^3)
Struvite	6.945	6.136	11.208	477.58
Potassium struvite	6.879	6.163	11.100	470.63

X-Ray powder diffraction data

	Struvite ($NH_4MgPO_4 \cdot 6H_2O$)		Potassium struvite ($KMgPO_4 \cdot 6H_2O$)	
hkl	*d*-spacing	Relative intensity	*d*-spacing	Relative intensity
110	5.905	40	5.846	10
020	5.601	60	5.551	25
011	5.378	25	5.390	18
111	4.257	100	4.241	100
021	4.139	40	4.123	60
200	3.475	12	3.436	20
130	3.289	25	3.258	39
201	3.022	14	2.969	18
130	3.289	25	3.258	39
201	3.022	14	2.969	18
012	2.958	25	2.923	16
211	2.919	55	2.899	64
040	2.802	35	2.774	37
112	2.722	16	2.726	10
022	2.690	50	2.695	55
221	2.660	45	2.642	45
231	2.452	12	2.332	12

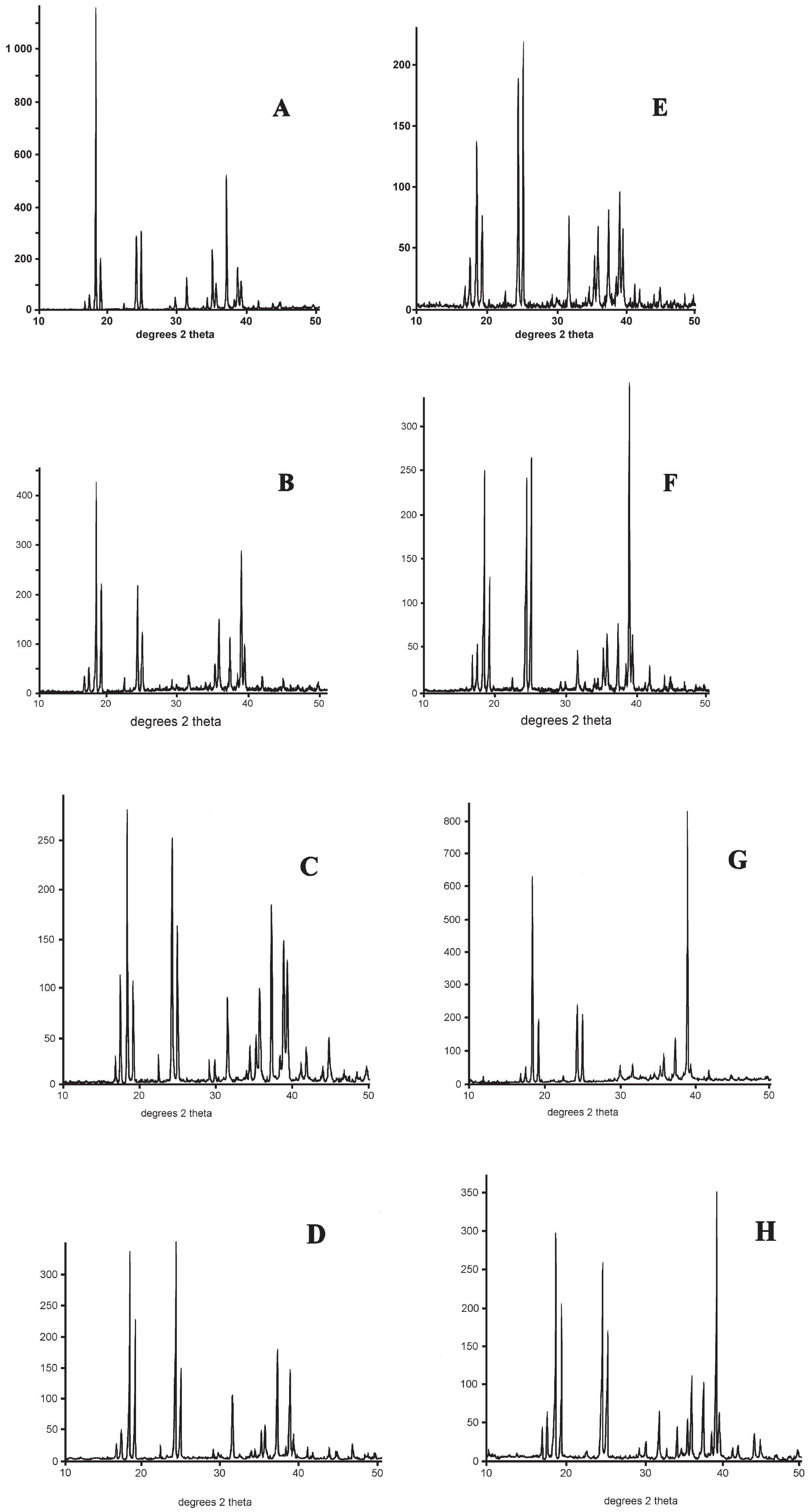

Fig. A. Eight examples of observed X-ray powder diffraction patterns of struvite calculi. In all cases, the *d*-spacings (values of 2θ) are the same for the important lines, but the relative intensities vary greatly. In **A** the peak at 19° is far higher than the pair at 24° 2θ. In **E** the situation is reversed; the pair at 24° is the strongest. In **F**, **G** and **H** the line at 39° 2θ is the strongest, whereas in **A** this line is far weaker than the line at 37°. These anomalous intensities can make identifying the calculus as struvite difficult if only the three or four strongest lines are used as the criterion in searching the Powder Diffraction File. Using the seven strongest lines, and ignoring the relative intensities, normally will identify the species as struvite. None of the scans **A–H** has obvious high backgrounds, nor are there the broad peaks due to poorly crystalline hydroxyl apatite (2.81–2.72 Å; 37–38° 2θ).

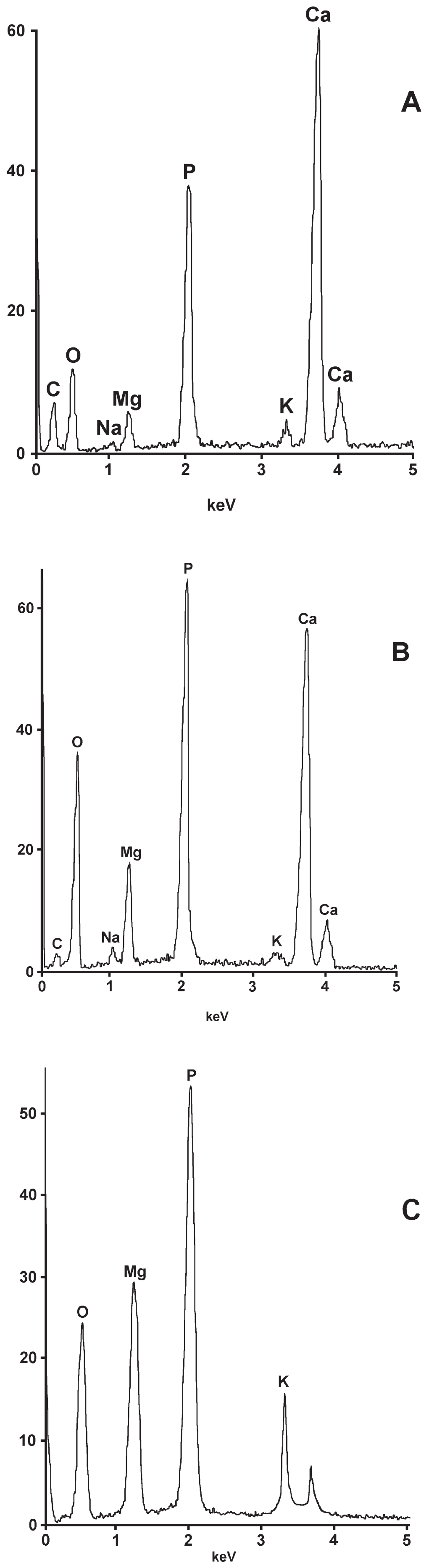

Fig. B. Scanning electron microscope EDAX data. These three scans illustrate typical results identifying the elements present in a calculus. **A**) Almost pure hydroxyl apatite; removed from the heart of a struvite stone. The presence of the hydroxyl apatite suggests that the animal may have a parathyroid problem, possibly hyperparathyroidism. **B**) Typical mixed intergrowth of materials. The solid hydroxyl apatite irritates the bladder, leading to infection by *Proteus*, the production of ammonia and the subsequent increase in pH which promotes the crystallization of struvite to form a large calculus. **C**) Almost pure struvite showing the presence of potassium. The potassium cation can be incorporated into the crystal structure in place of the ammonium cations, which have the same radius (i.e. isomorphous replacement).

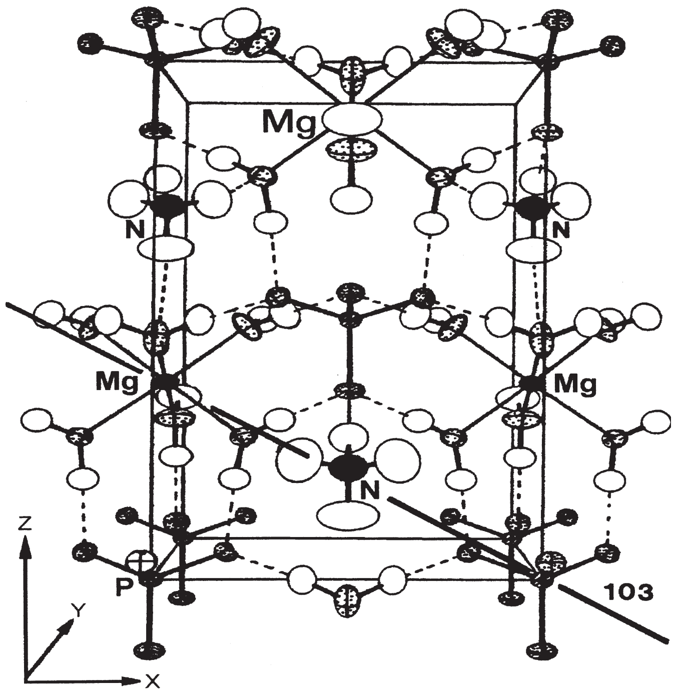

Fig. C. Projection of the struvite crystal structure along the *b*-axis (taken from ref. 7, Fig. 1), showing that the site occupied by the NH_4^+ ions lies on the 101, 103, 200 and 002 planes. The trace of the 103 plane is marked; note how it includes the Mg, N and P atoms.

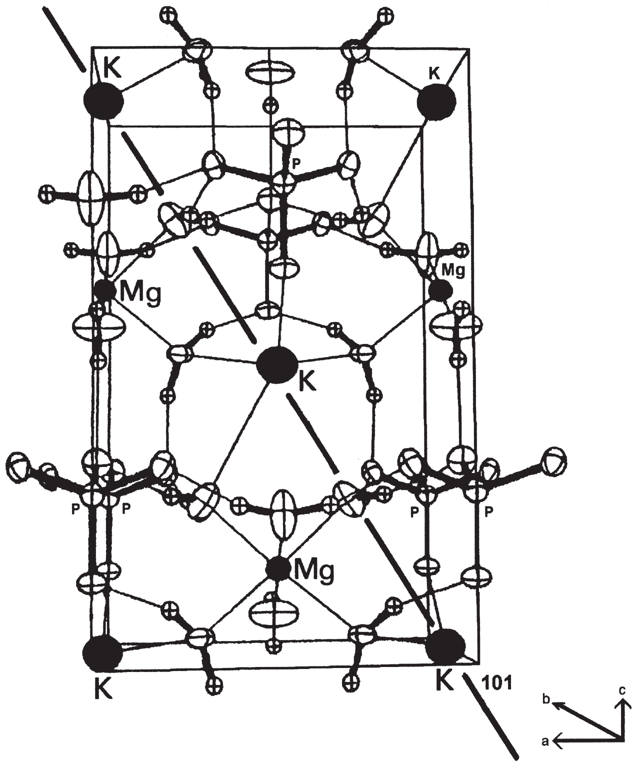

Fig. D. Projection of the crystal structure of the potassium analogue of struvite along the *b*-axis (taken from ref. 6, Fig 1) rotated 180° in the plane of the paper. It shows that the sites occupied by the K^+ ion which, like the NH_4^+ ion, lie on the 101, 103, 200, and 002 planes, and diffraction from these planes should be most affected by the replacement of NH_4^+ by K^+. The trace of the 101 plane through the K^+ ions is marked. The potassium ion (K^+) corresponds in space with the ammonium ion (NH_4^+) in Fig. 2.